

## Deuterium Relaxation in a Uniformly $^{15}\text{N}$ -Labeled Homeodomain and Its DNA Complex<sup>1</sup>

Konstantin Pervushin, Gerhard Wider, and Kurt Wüthrich\*

Institut für Molekularbiologie und Biophysik  
Eidgenössische Technische Hochschule Hönggerberg  
CH-8093 Zürich, Switzerland

Received December 16, 1996

Experimental<sup>2</sup> and theoretical<sup>3</sup> studies indicate that recognition of DNA sequences by proteins in transcriptional control may involve complex dynamics of amino acid side chains that mediate specificity of the interaction. Asparagine and glutamine are often implicated in such roles, so that direct experimental observation of the side chain mobility of these residues is of keen interest. Here we introduce 2D heteronuclear correlation experiments for studies of transverse and longitudinal deuterium relaxation of Asn and Gln in uniformly  $^{15}\text{N}$ -labeled proteins, which allow side chain dynamics to be described on the basis of the deuterium relaxation times and individual assignments of the *cis* (*Z*) and *trans* (*E*) amide hydrogens. These experiments contain important elements that were previously used by Kay and co-workers for studies on  $^{13}\text{C}$ - $^2\text{H}$  relaxation.<sup>4</sup> The  $^{15}\text{NH}_2$  groups are labeled to the extent of 50% with  $^2\text{H}$  by dissolving the protein or the protein–DNA complex in a 1:1 mixture of  $^2\text{H}_2\text{O}$  and  $^1\text{H}_2\text{O}$ . To prevent undesirable interference of NMR signals from the different species in such solutions, the magnetizations from the  $^{15}\text{N}^1\text{H}_2$  and  $^{15}\text{N}^2\text{H}_2$  moieties are filtered out by the pulse sequence. This approach was used with the uniformly  $^{15}\text{N}$ -labeled 70-residue *ftz* homeodomain<sup>5</sup> and its complex with an unlabeled 14-base pair DNA duplex that represents the BS2 operator site. The amino acid sequence of the *ftz* homeodomain contains seven Asn and Gln residues. Among these, Gln50 and Asn51 are highly conserved, and key roles in DNA recognition were previously attributed to these two residues from genetic and biochemical experiments.<sup>6</sup>

The pulse sequences proposed for measurements of the decay rates of  $^2\text{H}$  coherences (Figure 1; *I*, *N*, and *D* are the spin operators for  $^1\text{H}$ ,  $^{15}\text{N}$ , and  $^2\text{H}$ , respectively) include preparation of  $I_z N_y$  coherence at time point a, followed by transfer to  $D_z N_y$  at time b.  $D_z N_y$  is then converted to either deuterium antiphase coherence,  $D_x N_z$ , or two-spin order,  $D_z N_z$  (Figure 1), and the decay of these states is monitored during a delay *T* (the relaxation rate is evaluated from a series of measurements with different *T* values). The resulting spin states are transferred back to  $I_z N_y$  coherence, which evolves during  $t_1$  and is detected as proton magnetization after a sensitivity enhancement step.<sup>7</sup> The transfer of  $I_z N_y$  to  $D_z N_y$  is twice as fast for  $^2\text{H}$  as for spin 1/2 nuclei.<sup>8</sup> At time point c the polarization transferred back to  $^{15}\text{N}$  has the form  $D_z^2 I_z N_y$ , which corresponds to 2/3 of the

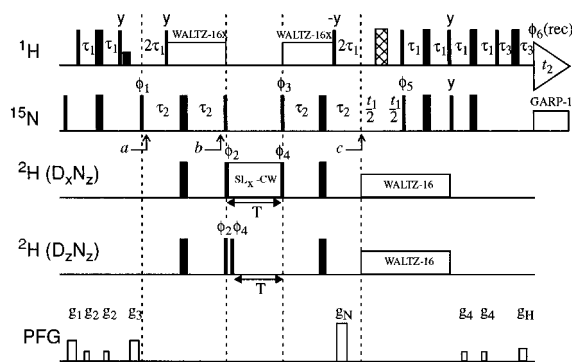


**Figure 1.** Experimental scheme for measuring relaxation rates of deuterium antiphase coherence,  $D_x N_z$ , and two-spin order,  $D_z N_z$ , in  $^1\text{H}$ – $^{15}\text{N}$ – $^2\text{H}$  spin systems. Narrow bars indicate  $90^\circ$  pulses and wide bars  $180^\circ$  pulses applied at the  $^1\text{H}$ ,  $^2\text{H}$ , or  $^{15}\text{N}$  frequencies. In a given experiment either the line labeled  $^2\text{H}(D_x N_z)$  nor the line  $^2\text{H}(D_z N_z)$  is used. The cross-hatched bar on the proton channel represents a composite ( $90_y$ – $220_x$ – $90_y$ ) inversion pulse.<sup>15</sup> Time points a, b, and c are indicated by arrows. To minimize saturation of the water signal, a selective rectangular  $^1\text{H}$  pulse of 2 ms duration is employed before a to return the magnetization to the *z*-axis. Subsequently, the water magnetization is rotated to the *x*-axis with a *y*-pulse and locked with a WALTZ-16 field. The deviation of the water magnetization from the transverse plane due to radiation damping during the short deuterium relaxation delays, *T*, can be neglected. The  $-y$ -pulse after the second WALTZ-16 irradiation returns the magnetization to the *z*-axis where it stays for the remainder of the pulse sequence. In  $^{15}\text{N}$  evolution and the subsequent polarization transfer period,  $^2\text{H}$  was decoupled with a 520 Hz WALTZ-16 sequence.<sup>16</sup>  $^1\text{H}$  and  $^{15}\text{N}$  decoupling were performed using 4.8 kHz WALTZ-16 and 1.8 kHz GARP-1 sequences,<sup>16</sup> respectively. A 2.1 kHz field was used for  $90^\circ$  and  $180^\circ$  pulses on  $^2\text{H}$ , and for spin-locking of the antiphase deuterium magnetization. The following delays were used:  $\tau_1 = 2.6$  ms,  $\tau_2 = 6$  ms, and  $\tau_3 = 1$  ms.  $2\tau_2$  was set shorter than  $1/4 J_{\text{DN}}$  to maximize magnetization transfer in the presence of deuterium relaxation. The offset frequencies of the  $^1\text{H}$ ,  $^2\text{H}$ , and  $^{15}\text{N}$  channels were placed at 4.8, 7, and 107 ppm, respectively. The phases of the rf-pulses were *x* unless specifically indicated:  $\phi_1 = (x, -x)$ ;  $\phi_2 = (2y, 2-y)$ ;  $\phi_3 = (8x, 8-x)$ ;  $\phi_4 = (4y, 4-y)$ ;  $\phi_5 = x$ ;  $\phi_6(\text{rec}) = [(x, -x, -x, x), 2(-x, x, x, -x), (x, -x, -x, x)]$ . For each value of  $t_1$  two FIDs were acquired, with the sign of  $g_N$  and the phase  $\phi_5$  inverted in the second FID. The duration and strength of the PFGs are as follows:  $g_1$  (1 ms, 30 G/cm);  $g_2$  (0.5 ms, 6 G/cm);  $g_3$  (1.05 ms, 30 G/cm);  $g_4$  (0.6 ms, 6 G/cm);  $g_N$  (1.25 ms, 60 G/cm);  $g_H$  (0.8 ms, 9.47 G/cm). Throughout the experiment the magnetic field  $\mathbf{B}_0$  was stabilized by the standard deuterium lock. Lock sampling was interrupted just before the first  $^2\text{H}$  pulse and resumed after the acquisition of the FID. (As an alternative the  $^{15}\text{N}$  evolution could be placed in the constant time period  $\tau_2$  for the back-transfer from  $D_z N_y$  to  $I_z N_y$ . However, the maximal  $^{15}\text{N}$  evolution time is then restricted to  $\tau_2 = 6$  ms, which is too short to resolve the small dispersion of the  $^{15}\text{N}$  chemical shifts of the side chains of Asn and Gln in the free *ftz* homeodomain (Figure 2).)

maximal magnetization transfer in a system consisting exclusively of spins 1/2.<sup>8</sup> Including losses due to  $^2\text{H}$  relaxation, the magnetization transfer to  $^2\text{H}$  and back to  $^{15}\text{N}$  leads to signal attenuation by a factor of  $(2/3) \exp(-4\tau_2/T_1)$ , which is  $\sim 0.1$  if the value of 12 ms measured for the *ftz* homeodomain is used for the longitudinal deuterium relaxation time  $T_1$  at 750 MHz. For medium-size and large-size proteins the sensitivity of this type of experiment will increase with  $\mathbf{B}_0$  since  $T_1$  increases with  $(\mathbf{B}_0)^2$ . The overall relaxation of the  $\{^2\text{H}, ^{15}\text{N}\}$  spin states can be approximated by the sum of the relaxation rates of each of the two spins:  $R(D_i N_z) \approx R(D_i) + R(N_z)$ ,  $i = x, z$ .<sup>4</sup>  $^{15}\text{N}$  longitudinal relaxation,  $R(N_z)$ , is slow compared to  $R(D_i)$  and contributes less than 0.1% to  $R(D_x N_z)$  and less than 1% to

(1) Abbreviations: NMR, nuclear magnetic resonance; 2D, two-dimensional; FID, free induction decay; PFG, pulsed field gradient; *ftz*, *fushi tarazu*.

(2) (a) Qian, Y. Q.; Otting, G.; Wüthrich, K. *J. Am. Chem. Soc.* **1993**, *115*, 1189. (b) Billeter, M.; Qian, Y. Q.; Otting, G.; Müller, M.; Gehring, W. J.; Wüthrich, K. *J. Mol. Biol.* **1993**, *234*, 1084. (c) Wilson, D. S.; Guenther, B.; Desplan, C.; Kuriyan, J. *Cell* **1995**, *82*, 709. (d) Hegte, R. S.; Grossman, S. R.; Laimins, L. A.; Sigler, P. B. *Nature* **1992**, *359*, 505. (e) Joachimiak, A.; Haran, T. E.; Sigler, P. B. *EMBO J.* **1994**, *13*, 367. (f) Gewirth, D. T.; Sigler, P. B. *Struct. Biol.* **1995**, *2*, 386. (g) Hirsch, J. A.; Aggarwal, A. K. *EMBO J.* **1995**, *14*, 6280.

(3) Billeter, M.; Güntert, P.; Luginbühl, P.; Wüthrich, K. *Cell* **1996**, *85*, 1057.

(4) Muhandiram, D. R.; Yamazaki, T.; Sykes, B. D.; Kay, L. E. *J. Am. Chem. Soc.* **1995**, *117*, 11536.

(5) Qian, Y. Q.; Furukubo-Tokunaga, K.; Resendez-Perez, D.; Müller, M.; Gehring, W. J.; Wüthrich, K. *J. Mol. Biol.* **1994**, *238*, 333.

(6) Gering, W. J.; Qian, Y. Q.; Billeter, M.; Furukubo-Tokunaga, K.; Schier, A. F.; Resendez-Perez, D.; Affolter, M.; Otting, G.; Wüthrich, K. *Cell* **1994**, *78*, 211.

(7) Cavanagh, J.; Palmer, A. G.; Wright, P. E.; Rance, M. *J. Magn. Reson.* **1991**, *91*, 429.

(8) Sørensen, O. W.; Eich, G. W.; Levitt, M. H.; Bodenhausen, G.; Ernst, R. R. *Prog. NMR Spectrosc.* **1983**, *16*, 163.

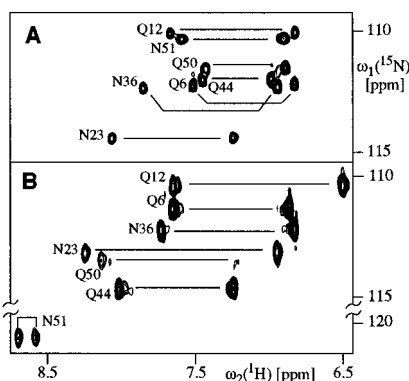


**Figure 2.**  $^1\text{H}$ ,  $^2\text{H}$ ,  $^{15}\text{N}$  correlation spectra obtained using the pulse sequence of Figure 1 with  $T = 100 \mu\text{s}$ : (A) 6 mM uniformly  $^{15}\text{N}$ -labeled *ftz* homeodomain at 18 °C; (B) 2 mM uniformly  $^{15}\text{N}$ -labeled *ftz* homeodomain in a complex with unlabeled DNA at 36 °C. For both measurements, the solvent was 45%  $\text{H}_2\text{O}/55\%$   $^2\text{H}_2\text{O}$ , pH 6.0, and the  $^1\text{H}$  frequency 750 MHz. For (A) the total measuring time was 2.2 h; 60 complex  $t_1$  points were acquired, with acquisition times of 24 and 51 ms in  $t_1$  and  $t_2$ , respectively. For (B) the total experimental time was 5.5 h; 60 complex  $t_1$  points were acquired, with acquisition times of 17 and 73 ms in  $t_1$  and  $t_2$ , respectively.

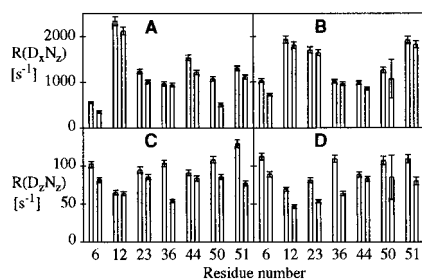


**Figure 3.** Relaxation rates of deuterium antiphase coherence,  $D_x N_z$ , (A, B), and of two-spin order,  $D_z N_z$ , (C, D), for the Asn and Gln side chain amide groups of the *ftz* homeodomain (A, C) and its DNA complex (B, D). For each residue the left and right bars represent the relaxation rates measured for the cross-peaks with the lower-field and higher-field proton resonances, respectively. To obtain the relaxation rates, 8–10 spectra of the type of Figure 2 were collected, using the pulse sequence of Figure 1 with variable delays  $T$  from 100  $\mu\text{s}$  to 12 ms.

$R(D_z N_z)$ . We therefore ignore  $R(N_z)$  and assume that  $R(D_i N_z) \approx R(D_i)$  holds with an accuracy better than 1%, with  $i = x, z$ .

In mixed solvents of  $^1\text{H}_2\text{O}$  and  $^2\text{H}_2\text{O}$ , four different amide moieties for a particular Asn or Gln side chain can be identified, *i.e.*, fully protonated, fully deuterated, or deuterated either at the *Z* or the *E* position. To maximize the concentration of the singly deuterated moieties, a slight excess of  $^2\text{H}_2\text{O}$  is required due to the preference for  $^1\text{H}$  binding to amide nitrogens observed for proteins.<sup>9</sup> Figure 2 shows two  $^1\text{H}$ ,  $^2\text{H}$ ,  $^{15}\text{N}$  correlation spectra of the *ftz* homeodomain and its DNA complex in a mixed solvent of 45%  $^1\text{H}_2\text{O}$  and 55%  $^2\text{H}_2\text{O}$  recorded at 750 MHz with the pulse sequence of Figure 1, using the line labeled  $^2\text{H}(D_x N_z)$  and  $T = 100 \mu\text{s}$ . Well-resolved spectra for the free protein as well as the protein–DNA complex were obtained for  $R(D_x N_z)$  and  $R(D_z N_z)$  measurements, so that all expected resonances of Asn and Gln residues can be clearly identified. A few  $^1\text{H}$ – $^{15}\text{N}$ – $^2\text{H}$  resonances of Arg residues were also observed, which are not further discussed in the present paper. Representative decay curves for measurements of  $R(D_x N_z)$  and  $R(D_z N_z)$  can be found as Supporting Information. The results for all Asn and Gln residues of the *ftz* homeodomain and its DNA complex are summarized in Figure 3. Measured transverse and longitudinal relaxation rates vary significantly for different residues. In all cases the transverse  $^2\text{H}$  relaxation rate manifested in the cross-peak with the lower-field  $^1\text{H}$  resonance (Figure 2; note that this

is the relaxation rate attributable to the higher-field  $^2\text{H}$  resonance) is larger than that manifested in the higher-field  $^1\text{H}$  peak (Figure 3). This observation was used to check on previous individual assignments of the proton resonances to the *E* and *Z* positions, which were based on the general observation in primary amides that the  $^1\text{H}^E$  proton is downfield of the  $^1\text{H}^Z$  proton.<sup>10</sup> An unambiguous assignment was thus obtained for all Asn and Gln residues, with the sole exception of Asn 36 where the difference between the two  $T_{1\rho}$  values is too small (Figure 3). Analyses of the molecular geometry of the side chain peptide groups determined by neutron diffraction at high resolution<sup>11</sup> show that the direction of the covalent bond between the amide nitrogen and  $^2\text{H}^Z$  is nearly parallel to the  $\text{C}^\beta$ – $\text{C}'$  bond in Asn, and parallel to the  $\text{C}'$ – $\text{C}^\delta$  bond in Gln. Since the direction of the principal component of the axially symmetric electric field tensor of  $^2\text{H}$  in amide groups is approximately parallel to the  $^{15}\text{N}$ – $^2\text{H}$  bond,<sup>12</sup> the relaxation of  $^2\text{H}^Z$  is thus largely insensitive to rotations about the dihedral angle  $\chi^2$  in Asn, or  $\chi^3$  in Gln, respectively.<sup>13</sup> In contrast,  $^2\text{H}^E$  has an effective additional degree of rotational freedom. In agreement with the experiments, theoretical models for description of multiple independent consecutive rotations in molecular structures<sup>13</sup> predict that the transverse relaxation rate  $R(D_x^E)$  should therefore be smaller than  $R(D_x^Z)$  for all macromolecular motional regimes at all reasonable magnetic field strengths for macromolecular NMR. The same statement cannot be made in such a general way for the longitudinal relaxation, although it holds for the data in Figure 3C,D. A corresponding effect was also observed for the amide  $^{15}\text{N}$  relaxation under conditions of broad band deuterium decoupling at sufficiently low magnetic field so that  $^{15}\text{N}$  relaxation by chemical shift anisotropy can be neglected (K. Pervushin, G. Wider, and K. Wüthrich, unpublished results).

In summary, the present experiments show that measurements of  $^2\text{H}$  relaxation in  $^1\text{H}$ – $^{15}\text{N}$ – $^2\text{H}$  spin systems in a mixed solvent of  $^1\text{H}_2\text{O}$  and  $^2\text{H}_2\text{O}$  are technically feasible. The NMR experiments used here will be applicable also to larger proteins because of their intrinsic high sensitivity at high magnetic fields. Deuterium relaxation data can effectively complement the more common  $^{15}\text{N}$  relaxation studies in the analysis of Gln and Asn side chain dynamics,<sup>14</sup> since  $^2\text{H}$  relaxation is dominated by the quadrupolar interaction, which can be characterized by a single directional vector. For each individual Asn or Gln side chain, information on internal mobility can thus be sampled by two different vectors. Thereby the analysis of the deuterium relaxation data is facilitated by the fact that relaxation of  $^2\text{H}^Z$  is insensitive to rotation about one of the dihedral angles (see above).

**Acknowledgment.** Financial support was obtained from the Schweizerischer Nationalfonds (Project 31.32033.91). We thank M. Wahl for the preparation of the *ftz* homeodomain and the *ftz*–DNA complex and Mrs. R. Hug for the careful processing of the manuscript.

**Supporting Information Available:** Figure S1 showing the experimental  $D_x N_z$  and  $D_z N_z$  decay curves (1 page). See any current masthead page for ordering and Internet access instructions.

JA964298Y

(10) (a) Piette, L. H.; Ray, J. D.; Ogg, Jr., R. A. *J. Mol. Spectrosc.* **1958**, *2*, 66. (b) Anet, F. A. L. and Bourn, A. J. R. *J. Am. Chem. Soc.* **1965**, *87*, 5250. (c) Redfield, A. G.; Waelder, S. *J. Am. Chem. Soc.* **1979**, *101*, 6151.

(11) (a) Verbist, J. J.; Lehmann, M. S.; Koetzle, T. F.; Hamilton, W. C. *Acta Crystallogr., B* **1973**, *29*, 2571. (b) Koetzle, T. F.; Frey, M. N.; Lehmann, M. S.; Hamilton, W. C. *Acta Crystallogr., B* **1973**, *29*, 2575.

(12) Mantsch, H. H.; Saito, H.; Smith, I. C. P. *Prog. NMR Spectrosc.* **1977**, *11*, 211.

(13) (a) Wallach, D. *J. Chem. Phys.* **1967**, *47*, 5258. (b) London, R. E.; Avitable, J. *J. Am. Chem. Soc.* **1978**, *100*, 7159.

(14) (a) Boyd, J. *J. Magn. Reson. B* **1995**, *107*, 279. (b) Buck, M.; Boyd, J.; Redfield, C.; MacKenzie, D. A.; Jeenes, D. J.; Archer, D. B.; Dobson, C. M. *Biochemistry* **1995**, *34*, 4041.

(15) Levitt, M. H. *Prog. NMR Spectrosc.* **1986**, *18*, 205.

(16) (a) Shaka, A. J.; Keeler, J.; Freeman, R. *J. Magn. Reson.* **1983**, *53*, 313. (b) Shaka, A. J.; Barker, P. B.; Freeman, R. *J. Magn. Reson.* **1985**, *64*, 547.